## 5.5 Crack Growth Prediction

The analysis procedure for crack-growth prediction requires the following steps:

1. Find baseline crack growth data (Section 5.1)
2. Select a retardation model; select and apply an integration routine (Section 5.2)
3. Establish a stress history and mission mix (Section 5.4)
4. Determine the stress-intensity factor (Section 11)

Each of these steps was discussed in general terms in one of the foregoing sections. However, there are some detail problems that need consideration. These detail problems are the subject of Section 5.5.

### 5.5.1 Cycle Definition and Sequencing

In Section 5.2, the retardation phenomenon was discussed. Retardation caused by high stress excursions can have a large effect on crack growth. As a result, the sequence of low and high stresses can be critical. Independent of retardation, however, there is another sequence effect that is related to the cycle definition necessary for a crack growth calculation.

If a flight-by-flight stress history is developed for damage tolerance analysis or tests, it will be given as a sequence of load levels. Each of the cases, *a*, *b*, c, and *d* in Figure 5.5.1, could be considered as a series of details in such a sequence. Each case is a stress excursion of $8\delta$ between levels A and B containing a dip of increasing size from *a* to *d*. In case *a*, the dip might be so small that for practical purposes it can be neglected. The cycle then can be considered as a single excursion with a range $\Delta K_1$ of size $8\delta$. In cases *b* through *d*, the dips are too big to be neglected. Normal crack growth calculations might consider each of these cases as a sequence of two excursions, for example case *b* would be made up of two excursions, one with a range $\Delta K_2$, the other with a range $\Delta K_3$, each of size $5\delta$.

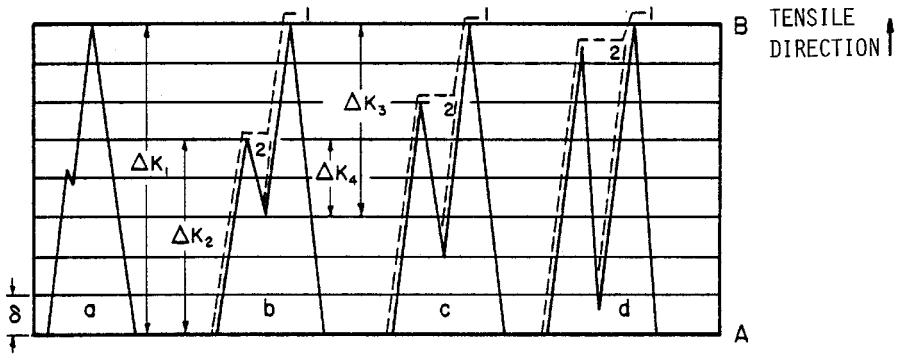


**Figure 5.5.1.** Definition of Cycles

**Table 5.5.1**. Calculation of Crack Growth For Figure 5.5.1

| | | | | |
|---|---|---|---|---|
| **Range Calculated Crack Growth ($\Delta a$)** | | | | |
| *a* | $\Delta a_a =$ | $C(\Delta K_1)^4 =$ | $C(8\delta)^4 =$ | $4096\ C\delta^4$ |
| *b* | $\Delta a_b =$ | $C(\Delta K_2)^4 + C(\Delta K_3)^4 =$ | $2C(5\delta)^4 =$ | $1250\ C\delta^4$ |
| *c* | $\Delta a_c =$ | | $2C(6\delta)^4 =$ | $2592\ C\delta^4$ |
| *d* | $\Delta a_d =$ | | $2C(7.5\delta)^4 =$ | $6328\ C\delta^4$ |
| **Range-Pair Calculated Crack Growth ($\Delta a$)** | | | | |
| *a* | $\Delta a_a =$ | $C(\Delta K_1)^4 =$ | $C(8\delta)^4 =$ | $4096\ C\delta^4$ |
| *b* | $\Delta a_b =$ | $C(\Delta K_1)^4 + C(\Delta K_4)^4 =$ | $C(8\delta)^4 + C(2\delta)^4 =$ | $4112\ C\delta^4$ |
| *c* | $\Delta a_c =$ | | $C(8\delta)^4 + C(4\delta)^4 =$ | $4352\ C\delta^4$ |
| *d* | $\Delta a_d =$ | | $C(8\delta)^4 + C(7\delta)^4 =$ | $6497\ C\delta^4$ |

If the four cases were treated this way, the calculated crack extension based on range excursions would be as given Table 5.5.1, where, for simplicity, the crack growth equation is taken as $da/dN = C(\Delta K)^4$ and the $R$ ratio effect is ignored. As indicated in this table, the damage estimates for cases *b* and *c* are considerably less than the crack damage estimated for case *a*. This is very unlikely in practice, since the crack would see one excursion from A to B in each case. Therefore, cases *b*, *c*, and *d* should be more damaging than case *a* in view of the extra cycle due to the dip. Although the effect of cycle ratio was neglected, the small influence of $R$ could not account for the discrepancies.

It seems more reasonable to treat each case as one excursion with a range of $\Delta K_1$ plus one excursion of a smaller range (e.g., $\Delta K_4$ in case *b*) which follows the philosophy of range-pair counting. If this is done, the ranges considered would be as indicated by the dashed lines in Figure 5.5.1. The crack growth calculation based on range-pair counting is shown at the bottom of Table 5.5.1, indicating an increasing amount of damage going from *a* to *d*.

Another cycle definition is obtained by rainflow counting [VanDÿk, 1972; Dowling, 1972]. The method is illustrated in Figure 5.5.2. While placing the graphical display of the stress history vertical, it is considered as a stack of roofs. Rain is assumed to flow from each roof. If it runs off the roof, it drips down the roof below, etc., with the exception that the rain does not continue on a roof that is already wet. The range of the rain flow is considered the range of the stress. The ranges so obtained are indicated by AB, CD, etc., in Figure 5.5.2. Figure 5.5.3 shows how cycle counting methods may affect a crack growth prediction.

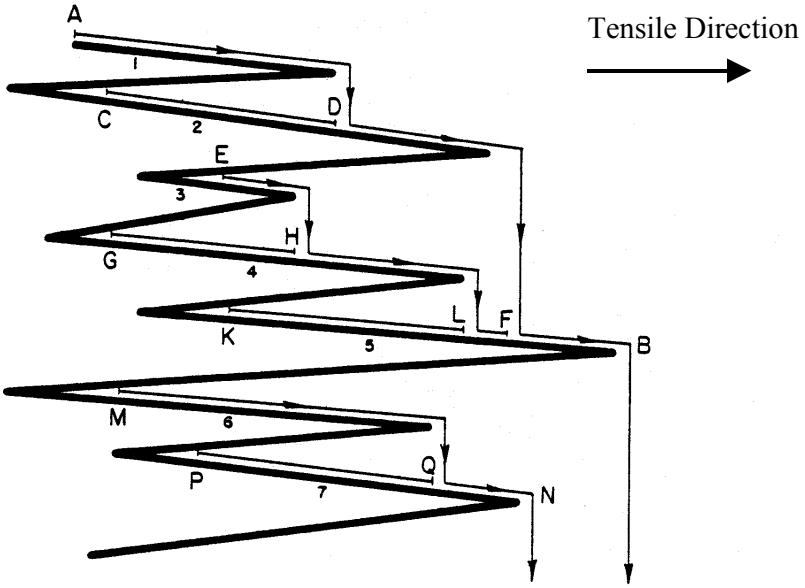


**Figure 5.5.2.** Rain Flow Count

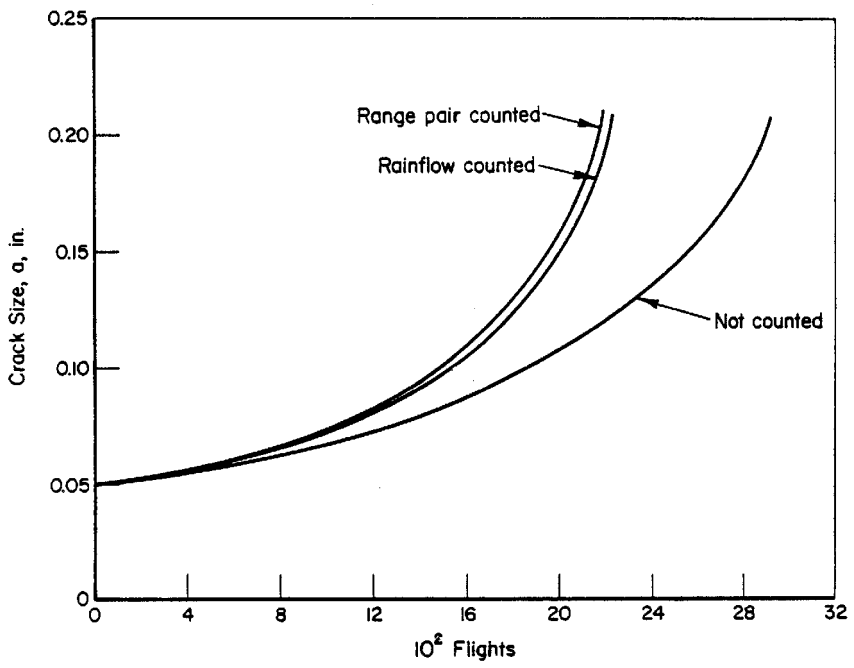


**Figure 5.5.3.** Calculated Crack Growth Curves for Random Flight-by-Flight Fighter Spectrum [VanDÿk, 1972]

Several other counting methods exist, and they are reviewed in Schijve [1963] and VanDÿk [1972]. Counting methods were originally developed to count measured load histories for

establishing an exceedance diagram. Therefore, the opinions expressed in the literature on the usefulness of the various counting procedures should be considered in that light. The counting procedure giving the best representation of a spectrum need not necessarily be the best descriptor of fatigue behavior.

It is argued that ranges are more important to fatigue behavior than load peaks. On this basis, the so-called range-pair count and the rainflow count are considered the most suitable. However, no crack growth experiments were ever reported to prove this.

The use of counting procedures in crack growth prediction is an entirely new application. An experimental program is required for a definitive evaluation. Calculated crack growth curves show that the difference in crack growth life may be on the order of 25-30 percent. It should be noted that counting is not as essential when the loads are sequenced low-high-low in each flight. The increasing ranges automatically produce an effect similar to counting.

For the time being, it seems that a cycle count will give the best representation of fatigue behavior. Therefore, it is recommended that cycle counting per flight be used for crack growth predictions of random sequences. Care should be taken that the stress ranges are sequenced properly to avoid different interaction effects (note that $K_{max}$ determines retardation and not $\Delta K$). As an example, consider again Figure 5.5.2. The proper sequence for integration is: CD, GH, KL, EF, AB, PQ, MN. In this way, the maximum stress intensity (at B) occurs at the proper time with respect to its retardation effect, and the maximum stress-intensity of cycle AB will cause retardation for cycles PQ and MN only.

### 5.5.2 Clipping

Apart from the sequencing problems addressed in the previous section, there is a sequence problem associated with retardation. In Section 5.4, it was pointed out that sequencing of deterministic loads should be done in accordance with service practice; probabilistic loads can be sequenced randomly, but a low-high-low order per flight is acceptable. This can be concluded from data of the type presented in Figure 5.2.5.

The sequencing effect due to retardation is largely dependent on the ratio between the highest and lowest loads in the spectrum and their frequency of occurrence. As a result, it will depend upon spectrum shape. Compare, for example, the fighter spectrum with the transport spectrum in Figure 5.4.6. The relatively few high loads in the transport spectrum may cause a more significant retardation effect than the many high loads in the fighter spectrum.

The selection of the highest loads in the load history is critical to obtain a reliable crack growth prediction. It was argued in Section 5.4 that it is not realistic to include loads that occur less frequently than about 10 times in 1,000 flights, because some aircraft in the force may not see these high loads. This means that the spectrum is clipped at 10 exceedances. No load cycles are omitted. Only those higher than the clipping level are reduced in magnitude to the clipping level. The effect of clipping on retardation and crack growth life was illustrated in Figure 5.2.4.

The question remains whether proper selection of a realistic clipping level is as important for a crack-growth prediction as it is for an experiment. In this respect, it is important to know which retardation model is the most sensitive to clipping level. As pointed out above, the sensitivity may also depend upon spectrum shape. The effects can be determined by running crack growth

calculations for different clipping levels, different spectrum shapes, and with two retardation models.

Calculations were made for the six spectra shown in Figure 5.4.6, by using the flight-by-flight history developed in Example 5.4.2. The cycles in each flight were ordered in a low-high-low sequence. Figure 5.5.4 shows the crack growth curves for the full spectra using the Willenborg model, and Figure 5.5.5 shows the curves using the Wheeler model. The crack configuration was a corner crack from a hole, as indicated in the figures. A limit load stress of 35 ksi was used for all spectra, and the material was 2024-T3 aluminum.

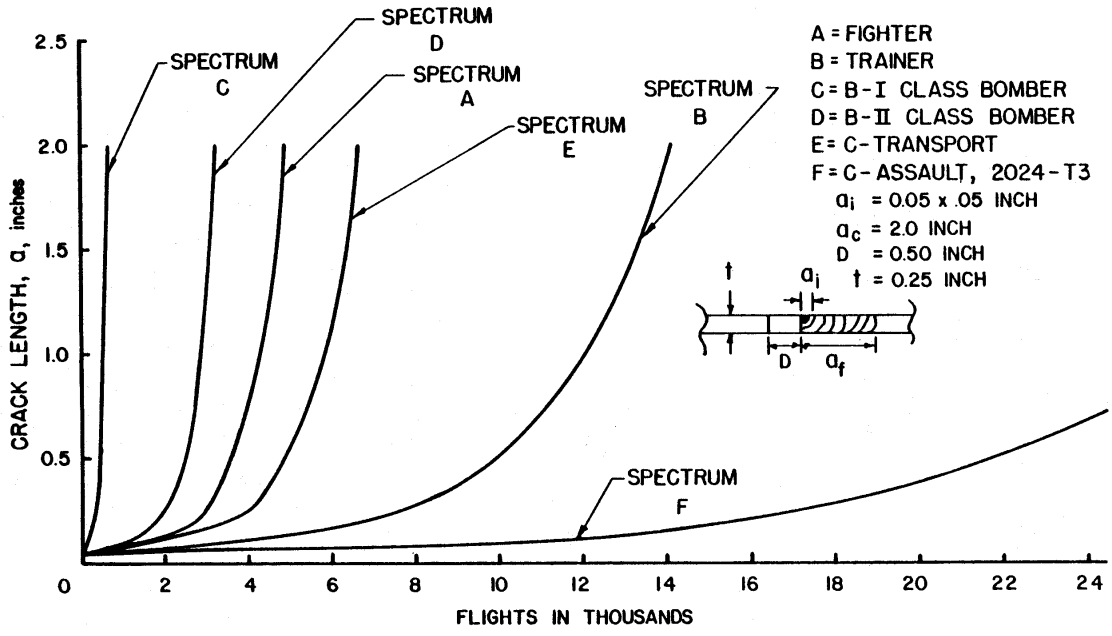


**Figure 5.5.4.** Spectrum Fatigue Crack Growth Behavior Willenborg Retardation Model

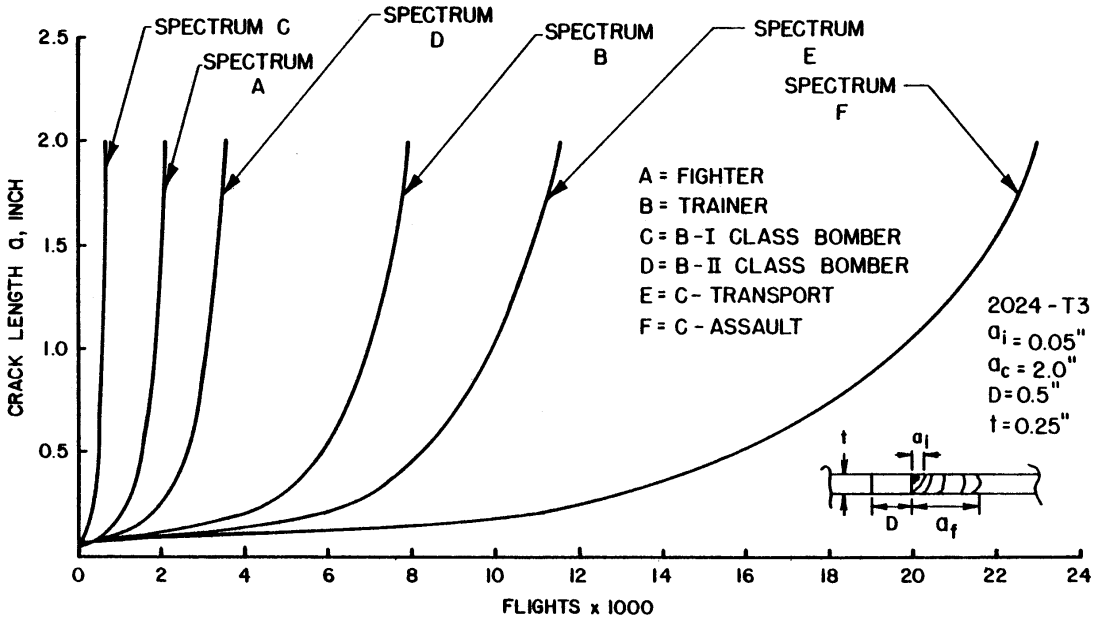


**Figure 5.5.5.** Spectrum Fatigue Crack Growth Behavior Wheeler Retardation Model

Subsequently, four significantly different spectra (A, B, C, and E) were selected. Crack growth curves were calculated using the clipping levels $S_2$, $S_3$, $S_4$, and $S_5$ in Example 5.4.2. The resulting crack growth curves for one spectrum are presented in Figure 5.5.6. Also shown is a curve for a linear analysis (no retardation). The crack growth life results for all spectra are summarized as a function of clipping level in Figure 5.5.7. Test data for gust spectrum truncation are also shown. Some characteristic numbers are tabulated in Table 5.5.2 for the four spectra as a function of crack growth model.

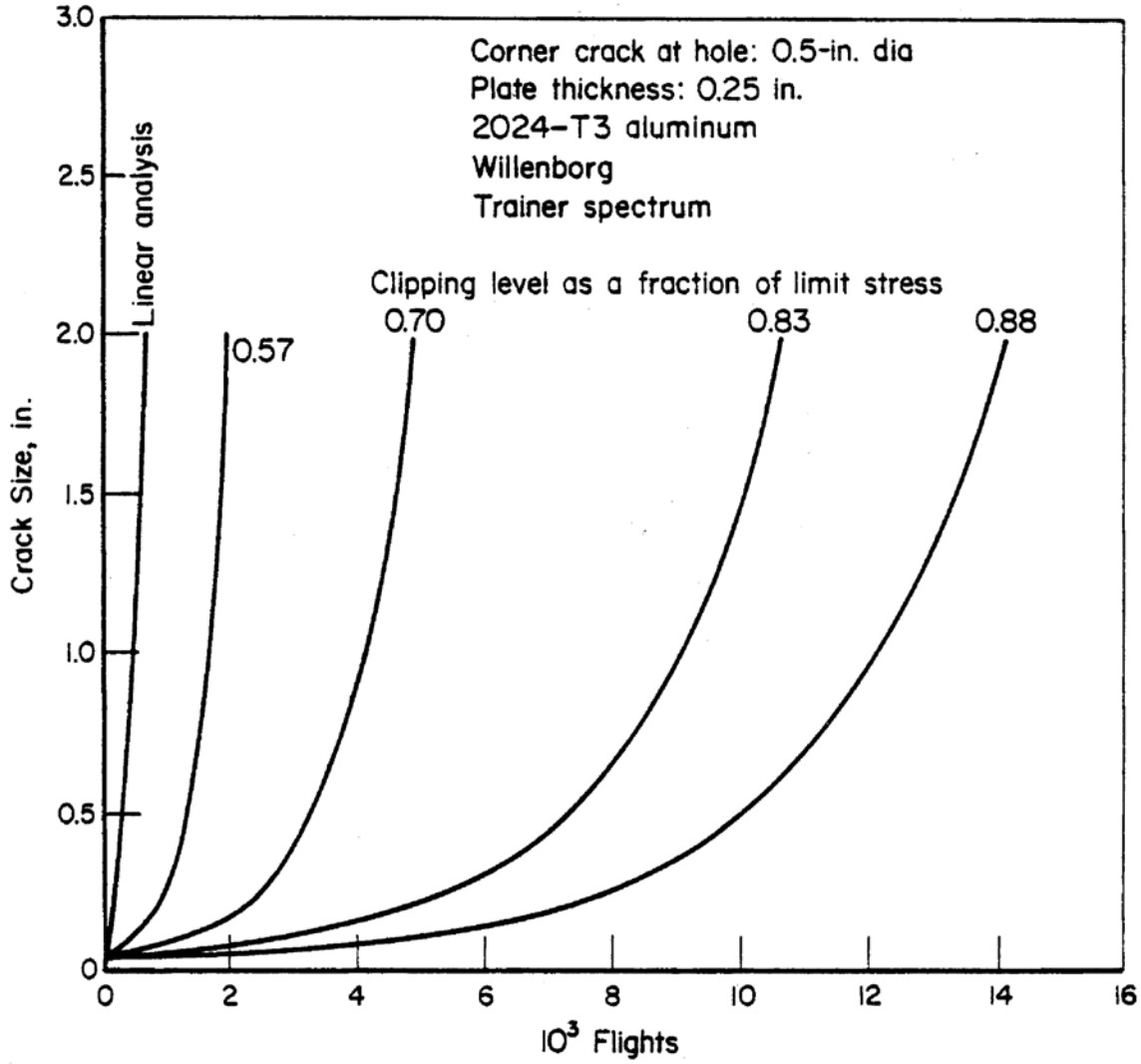


**Figure 5.5.6.** Effect of Clipping Level on Calculated Crack Growth for Spectrum B-Trainer

**Table 5.5.2.** Characteristic Value for the Four Spectra of Figure 5.5.6

| Symbol | Spectrum | Linear Analysis (Flights) | Retardation Life (Flights) | |
|---|---|---|---|---|
| | | | Willenborg Fully Retarded | Wheeler m = 2.3 |
| A ▲ Willenborg △ Wheeler | Fighter | 270 | 4,900 | 2,100 |
| B ● Willenborg ○ Wheeler | Trainer | 460 | 14,200 | 7,900 |
| C ■ Willenborg □ Wheeler | B-1 Class Bomber | 140 | 700 | 700 |
| D ▼Willenborg ▽ Wheeler | C Transport | 1,270 | 6,700 | 11,600 |

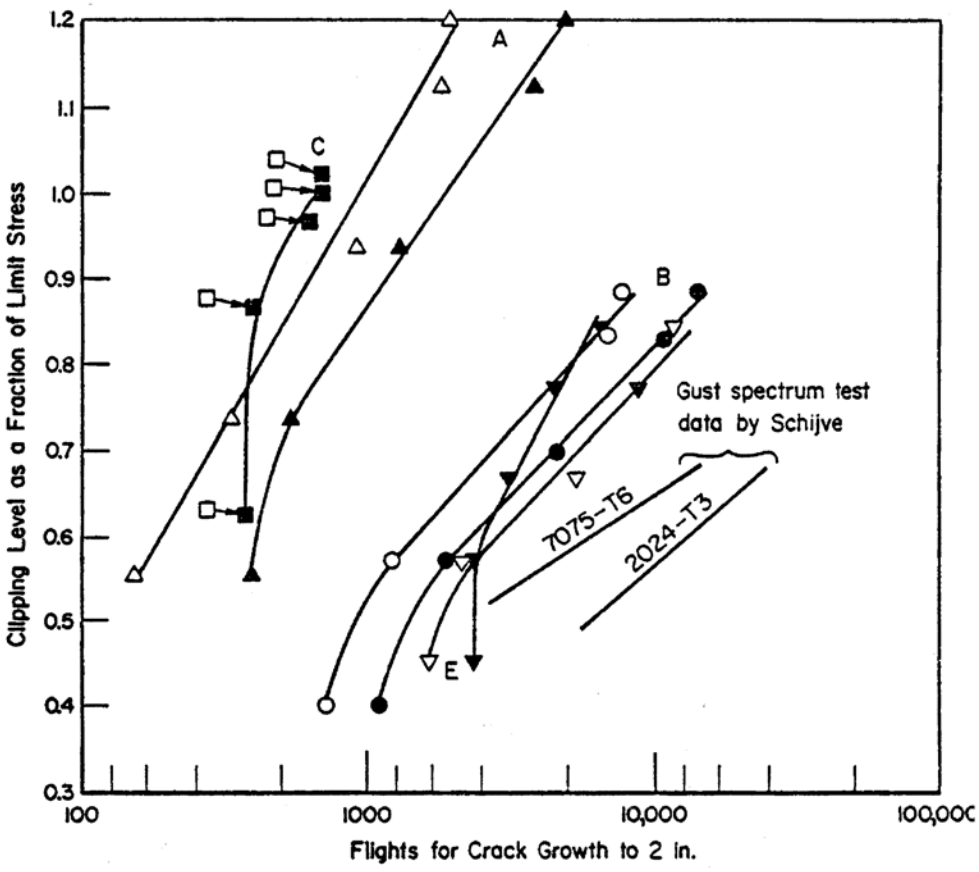


**Figure 5.5.7.** Effect of Clipping for Various Spectra

Figures 5.5.4 through 5.5.7 allow the following observations:

- The two retardation models predict largely different crack growth lives for all spectra, except C. The differences are not systematic. Since there are no test data for comparison, the correct answers are not known.
- With one exception, the two models essentially predict the same trend with respect to clipping levels. This shows that they both have equal capability to treat retardation.
- The steep spectra (fighter, trainer) are somewhat more sensitive to clipping level. Apparently, the damage of the high cycles outweighs their retardation effect.
- With extreme clipping, the analysis attains more the character of a linear analysis, indicating that the largest amount of damage in the linear analysis comes from the large number of smaller amplitude cycles.
- Bringing the clipping level down from 10 exceedances per 1,000 flights (top data points in Figure 5.5.7) to 100 exceedances per 1,000 flights (second row of data points in Figure 5.5.7) reduces the life by only 15 percent or less for all spectra.

In addition, crack growth calculations were made to re-predict the gust spectrum test data shown in Figure 5.5.7. The results are presented in Figure 5.5.8 where the calculated results are shown to be very conservative. However, with one exception, they would all fall within the scatter-band of Figure 5.2.4. The baseline data used were worst case upper-bound *da/dN* data. This can easily account for a factor of two in growth rates. If the growth rates were reduced by a factor of two, the calculations would be very close to the test data (dashed line in Figure 5.5.8).

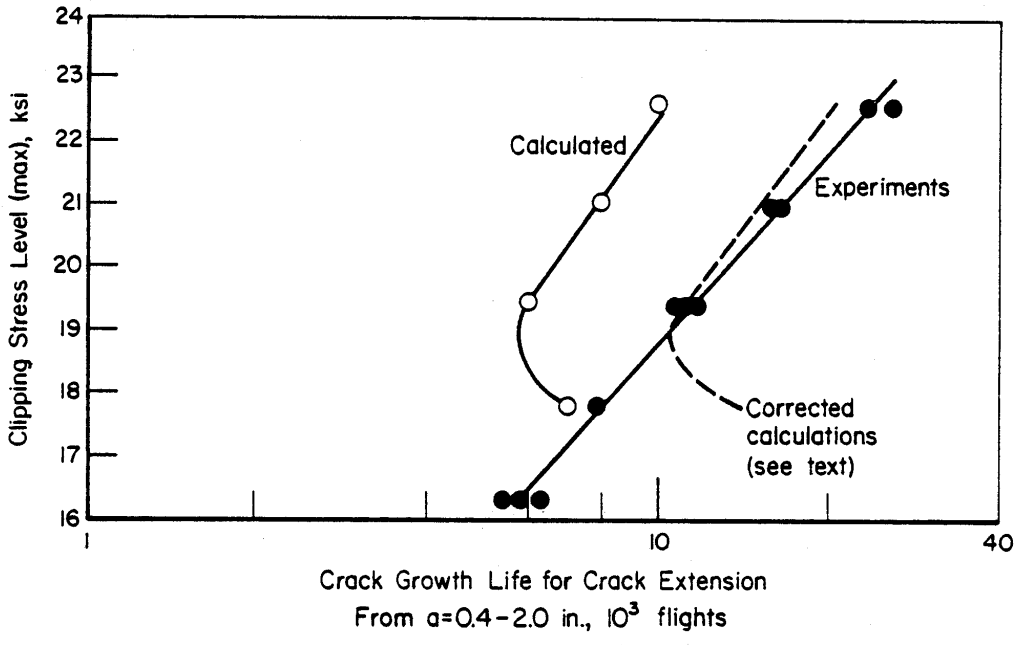


**Figure 5.5.8.** Calculated and Experimental Data for Gust Spectrum Clipping [Schijve, 1970; 1972]

One important thing has been disregarded so far. As shown in Figure 5.2.1, compressive stresses reduce retardation (compare curves B and C). Omission of the ground-air-ground (GAG) cycle in the experiments by Schijve (1970) shown in Figure 5.5.8 increased the life by almost 80 percent. Apart from the GAG cycle, there are other compressive stresses in the spectrum. All compressive stress effects were ignored in the crack growth calculations with the retardation models used for this analysis.

The top clipping level in Figure 5.5.8 is at 5 exceedances per 1,000 flights, the second level is at 13 exceedances per 1,000 flights. From these results and Figure 5.5.7, it appears that an exceedance level of 10 times per 1,000 flights will combine reasonable conservatism with a realistically high clipping level. This supports the arguments given previously to select the clipping level at 10 exceedances per 1,000 flights for both calculations and experiments. The effect of clipping level should be calculated for a small number of representative cases to show the degree of conservatism.

### 5.5.3 Truncation

Truncation of the lower load levels is important for the efficiency of crack growth calculations. Truncation means that cycles below a certain magnitude are simply omitted. The argument is that low stress excursions do not contribute much to crack growth, especially in view of the retardation effect. Since there are so many cycles of low amplitude, their omission would speed up experiments and crack growth calculations.

Figure 5.5.9 shows some experimental data regarding the effect of truncation. The lowest load levels of a complete stress history were simply omitted, without a correction of the stress history. These data might be somewhat misleading, because truncation was not carried out properly. Figure 5.5.10 shows the improper and the correct procedure for truncation.

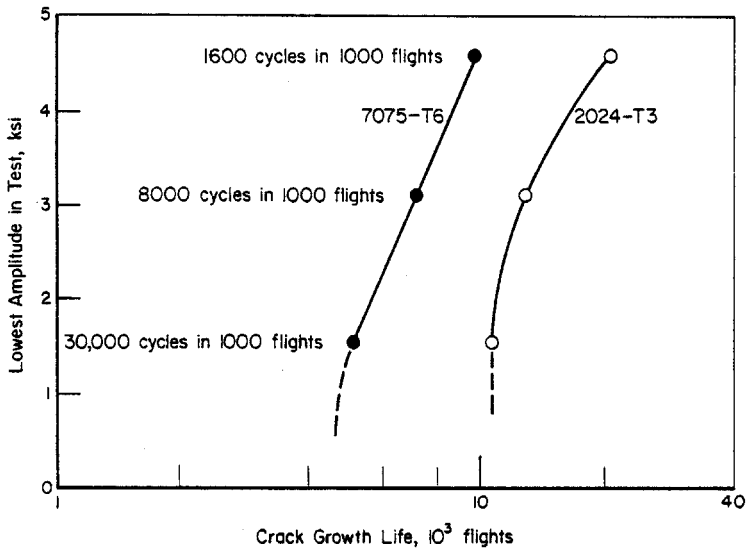


**Figure 5.5.9.** Effect of Lowest Stress Amplitude in Flight-by-Flight Tests Based on Gust Spectrum [Schijve 1970; 1972 ]

The left half of Figure 5.5.10 illustrates the truncation procedure used for the experiments in Figure 5.5.9. In the example, the 580,000 cycles of level $S_8$ would simply be omitted, thus reducing the total cycle content from 700,000 to 120,000. Proper truncation requires that the lower spectrum approximation step be reconstructed, as indicated in the right half of Figure 5.5.10. The hatched areas in the figure should be made equal. This means that the number of $S_7$ cycles would increase from 80,000 to 260,000, and the total cycle content would be reduced from 700,000 to 300,000. This increase of 180,000 cycles of $S_7$ would be substituted for 580,000 cycles of $S_8$. In this way, the effects of lower level truncation are less than suggested by the experimental data in Figure 5.5.9.

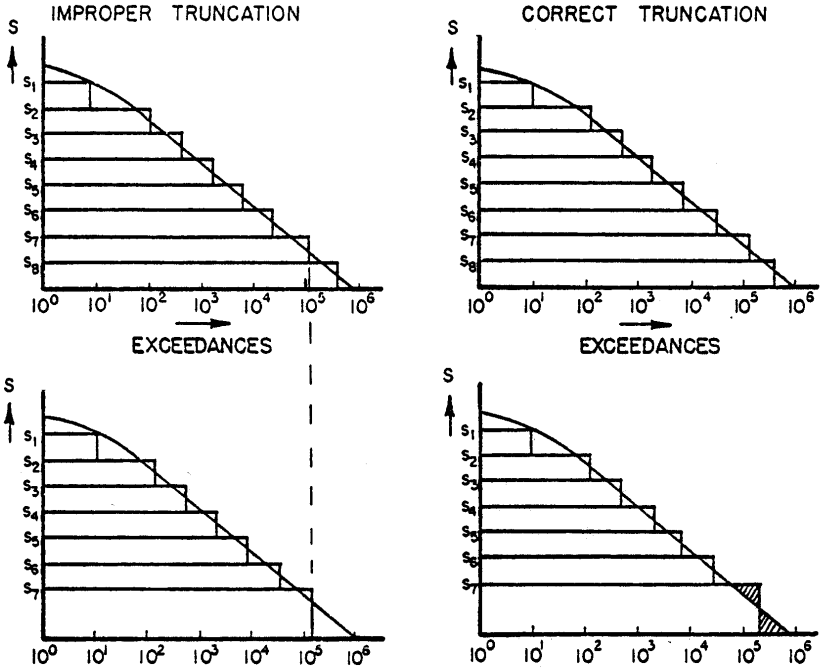


| Improper Truncation | | |
|---|---|---|
| **Level** | **Exceedances** | **Occurrences** |
| $S_1$ | 10 | 10 |
| $S_2$ | 100 | 90 |
| $S_3$ | 600 | 500 |
| $S_4$ | 2,000 | 1,400 |
| $S_5$ | 8,000 | 6,000 |
| $S_6$ | 40,000 | 32,000 |
| $S_7$ | 120,000 | 80,000 |
| $S_8$ | 700,000 | 580,000 |

| Correct Truncation | | |
|---|---|---|
| **Level** | **Exceedances** | **Occurrences** |
| $S_1$ | 10 | 10 |
| $S_2$ | 100 | 90 |
| $S_3$ | 600 | 500 |
| $S_4$ | 2,000 | 1,400 |
| $S_5$ | 8,000 | 6,000 |
| $S_6$ | 40,000 | 32,000 |
| $S_7$ | 300,000 | 260,000 |

**Figure 5.5.10.** Improper and Correct Truncation

In Section 5.4 it was recommended that the truncation level be selected at $10^5$ - $5x10^5$ exceedances per 1,000 flights, depending upon how steep the exceedance curve is at its extreme point. That recommendation is reiterated here.

### 5.5.4 Crack Shape

The most common crack shape in crack growth analysis is the quarter-circular corner flaw at the edge of a hole. Stress-intensity factor solutions for this case are presented in Section 11. For use in crack growth analysis, these solutions present some additional problems. The stress-intensity factor varies along the periphery of the crack. Since crack growth is a function of the stress-intensity factor, crack extension also will vary along the crack front. If this is accounted for in a calculation, the flaw shape at a hole changes from quarter-circular to quarter-elliptical.

For the calculation, it would be sufficient to include two points of the crack front, e.g., the crack tip at the surface and the crack tip at the edge of the hole. The stress-intensity factor is calculated at these points, and the amount of crack growth determined. There will be a different amount of growth along the surface than along the edge of the hole. For an initially quarter-circular crack of size $a_i$, the new crack will have a size $a_i+\Delta a_s$ along the surface, and a size $a_i+\Delta a_h$ along the hole. For the next crack growth increment the crack may be considered a quarter-elliptical flaw with semi-axes $a_i+\Delta a_s$, and $a_i+\Delta a_h$.

There are three reasons why the above procedure may not give the accuracy expected for crack growth life estimating:

- The variation of stress-intensity factor along a corner flaw front at the edge of a hole is not accurately known.
- The differences in stress-intensity factor cause differences in growth and flaw shape development. If this is so, the difference in crack growth properties in the two directions (anisotropy) should be accounted for too.
- The differences in growth rates and stress-intensity factor levels also give different retardation effects.

When the flaw size becomes equal to the plate thickness, the flaw will become a through-thickness-crack with a curved front for which stress-intensity solutions are readily available. Cracks usually have a tendency to quickly become normal-through-thickness cracks once they reach the free surface (Figure 5.5.11). Therefore, it is recommended to conservatively assume the crack to become a normal-through-thickness-crack of a size equal to the thickness immediately after it reaches the free surface ($a = B$, Figure 5.5.11).

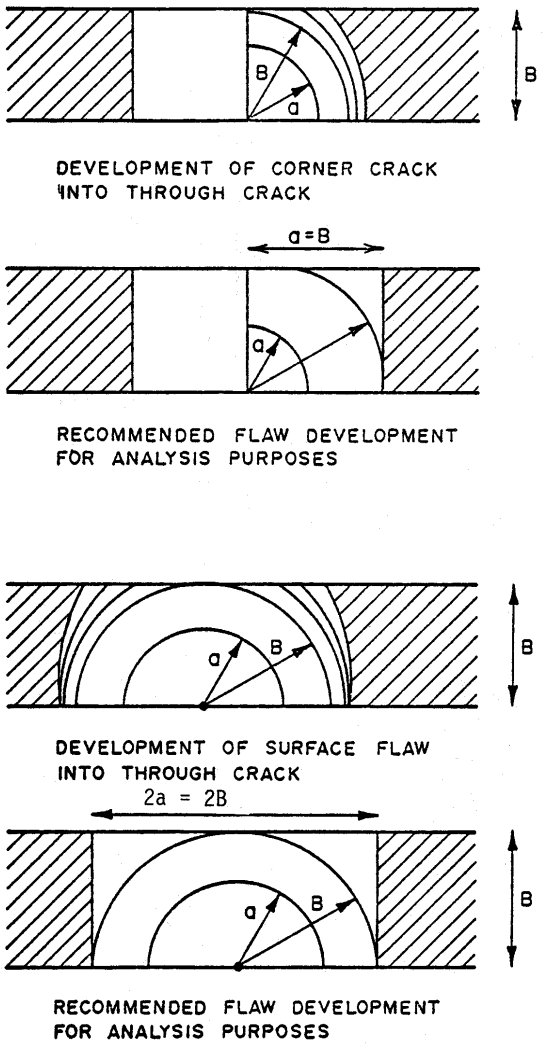


**Figure 5.5.11.** Development of Flaws

### 5.5.5 Interaction of Cracks

For the initial flaw assumptions, JSSG-2006 paragraph A3.12.1 states: "Only one initial flaw in the most critical hole and one initial flaw at a location other than a hole need be assumed to exist in any structural element. Interaction between these assumed initial flaws need not be considered." Obviously, interaction between these cracks can be disregarded because these cracks are not assumed to occur simultaneously, although each of them may occur separately. However, more than one initial flaw may occur if due to fabrication and assembly operations two or more adjacent elements can contain the same initial damage at the same location. Note that each of the adjacent elements has only one flaw. JSSG-2006 paragraph A3.12.1 further states: "For multiple and adjacent elements, the initial flaws need not be situated at the same location, except for structural elements where fabrication and assembly operations are conducted such that flaws in two or more elements can exist at the same location."

The previous statement that interaction between assumed initial flaws need not be considered is not repeated here because these cracks will interact as they occur simultaneously. In principle, the damage tolerance calculation should consider this interaction. However, a rigorous treatment of this problem is prohibitive in most cases. Consider, e.g., a skin with a reinforcement as in Figure 5.5.12. Because of assembly drilling, both holes should be assumed flawed (Figure 5.5.12a). If both elements carry the same stress, there will be hardly any load transfer initially. Hence, the stress intensities for both flaws will be equal, implying that initially both will grow at the same rate.

If the two cracks continue to grow simultaneously in a dependent manner, their stress-intensity factors ($K$) will eventually be different (e.g., $K$ of the reinforcement would increase faster if only for the finite size effect). This means that in a given cycle the rate of growth would be different for the two cracks resulting in different crack sizes. Since it cannot be foreseen prior how the crack sizes in the two members develop, it would be necessary to develop $K$-solutions for a range of crack sizes and a range of crack size ratios in the two members.

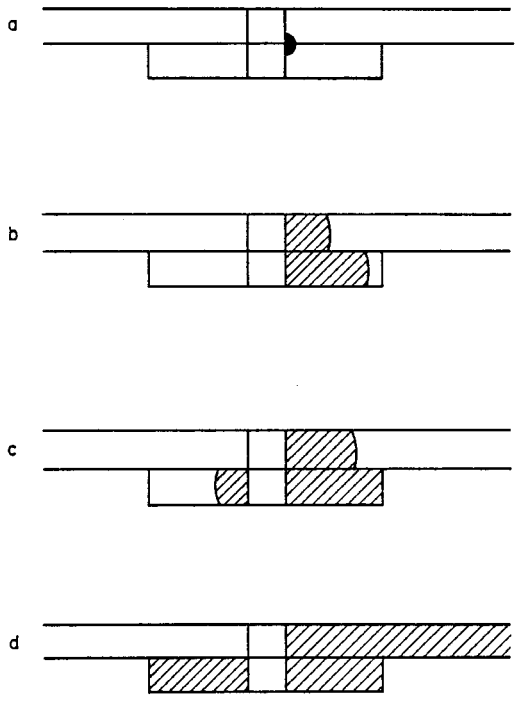


**Figure 5.5.12.** Interaction of Cracks

EXAMPLE 5.5.1: Interacting Cracks

Assume the crack size in the skin is $a_s$, the crack size in the reinforcement $a_r$. For a given value of $a_r$, the $K$ for the skin crack would be calculated as a function of $a_s$. This calculation would be repeated for a range of $a_r$ sizes. The same would be done for the reinforcement crack and a range of $a_s$ values. For any given combination of $a_r$ and $a_s$, the two stress-intensity factors then can be found by interpolation.

Although the consequences of crack interaction should be evaluated, routine calculations may be run without interaction of cracks [Smith, et al., 1975; Smith, 1974]. Obviously, the calculation procedure is much simpler if interaction can be ignored. However, the procedure may give unconservative results.

If either element remained uncracked, the stress-intensity factor in the cracked element would be much lower because there would be load transferred from the cracked element to the uncracked element. Obviously, the stress-intensity factor in the cracked skin of Example 5.5.1 would be the lowest. The cracks could be grown as if the other element was uncracked and crack growth would be slower.

Finally, the reinforcement could be totally cracked. Interaction must be taken into account, i.e., the crack in the skin would be treated now for the case of a failed reinforced panel (e.g., stringer reinforced structure with middle stringer failed).

This means that two analysis have to be made for a $K$-determination, one with the reinforcement uncracked, one with the reinforcement failed. If the two independent crack growth analyses show that the reinforcement has failed, the analysis of the skin is changed appropriately.